Remote Sensing of Environment 195 (2017) 297–312

Contents lists available at ScienceDirect

Remote Sensing of Environment

journal homepage: www.elsevier.com/locate/rse

A comparison of SMOS and AMSR2 soil moisture using representative sites of the OzNet monitoring network

Mei Sun Yee[a,*], Jeffrey P. Walker[a], Christoph Rüdiger[a], Robert M. Parinussa[b], Toshio Koike[c], Yann H. Kerr[d]

[a] Department of Civil Engineering, Monash University, Clayton, Australia
[b] School of Civil and Environmental Engineering, University of New South Wales, Sydney, Australia
[c] Department of Civil Engineering, School of Engineering, The University of Tokyo, Japan
[d] CESBIO-CNES-CNRS-IRD-Université Toulouse, Toulouse Cedex 9 31401, France

ARTICLE INFO

Article history:
Received 30 May 2016
Received in revised form 5 April 2017
Accepted 12 April 2017
Available online xxxx

Keywords:
Soil moisture
Representativeness
AMSR2
SMOS
JAXA
LPRM

ABSTRACT

This paper evaluates the performance of different soil moisture products from AMSR2 and SMOS against the most representative stations within the Yanco study area in the Murrumbidgee catchment, in southeast Australia. AMSR2 Level 3 (L3) soil moisture products retrieved from two versions of brightness temperatures using the Japanese Aerospace eXploration Agency (JAXA) and the Land Parameter Retrieval Model (LPRM) algorithm were included. For the LPRM algorithm, two different parameterization methods were applied. Furthermore, two versions of SMOS L3 soil moisture product were assessed. The results are contrasted against the use of "random" stations. Accounting for all versions, frequencies and overpasses, the latest versions of the JAXA (JX2) and LPRM (LP3) products were found to surpass the earlier versions (JX1, LP1 and LP2). Soil moisture retrieval based on the latter version of brightness temperature and parameterization scheme improved when C-band observations were used but not X-band. However, X-band retrievals (r: 0.71, MAE: 0.07, RMSD: 0.08 m^3/m^3) were found to perform better than C-band (r: 0.68–0.70, MAE: 0.07–0.09 m^3/m^3, RMSD: 0.09–0.10 m^3/m^3). Moreover, an intercomparison between different acquisition times (morning and evening) of AMSR2 X-band products found a better performance from evening overpasses (1:30 pm; r: 0.69–0.77) as opposed to morning overpasses (1:30 am; r: 0.47–0.66). In the case of SMOS, morning (6:00 am; r: 0.77) retrievals were found to be superior over evening (6:00 pm; r: 0.69) retrievals. Overall, both versions of JAXA products, the second and third versions of LPRM X-band products, and two versions of SMOS products were found to meet the mean average error (MAE) *goal accuracy* of the AMSR2 mission (MAE < 0.08 m^3/m^3) but none of the products achieved the SMOS goal of RMSD < 0.04 m^3/m^3. Furthermore, performance of the products differed depending on the statistic used to evaluate them. Consequently, considering the results in this study, JX2 products are recommended if both absolute and temporal accuracy of the soil moisture product is of importance, whereas $LP3_X$ products from evening observations and SMOS version 3.00 (SMOS2) products from morning overpasses are recommended if temporal accuracy is of greater importance.

1. Introduction

Soil moisture plays a key role in the Earth's water cycle by influencing how rainfall is partitioned into runoff, infiltration and ground water recharge; and the rate in which plants transpire. Therefore, incorporating soil moisture observations into models can improve weather forecasting (e.g. Draper, 2011, Drusch, 2007), climate modelling (e.g. Dirmeyer, 2000; Seneviratne, 2010), drought and flood predictions (e.g. Bindlish et al., 2009, Cai et al., 2009), and agriculture and water resource management. Whilst soil moisture information can be obtained through *in situ* or remote sensing methods, only remote sensing can provide observations at regional to global scales.

Recent advances in the remote sensing of soil moisture has increased the availability of soil moisture observations. The stark contrast between the dielectric constant of soil and water at microwave bands enables active and/or passive remote sensing observations to provide information on soil moisture content (Owe et al., 2008). Current space-borne soil moisture sensors operating at X- (e.g. 10.7 GHz) and/or C-band (e.g. 6.9 GHz) include the Advanced Microwave Scanning Radiometer (AMSR2) aboard the Global Change

* Corresponding author.
E-mail address: mei.yee@monash.edu (M.S. Yee).

http://dx.doi.org/10.1016/j.rse.2017.04.019
0034-4257/

Observation Mission-Water(GCOM-W1), and Advanced Scatterometer (ASCAT) on-board the Meteorological Operational (MetOp) series of satellites (Wagner et al., 2013). Operating at L-band (e.g. 1.4 GHz) are the Soil Moisture and Ocean Salinity (SMOS) (Kerr et al., 2012) and Soil Moisture Active Passive (SMAP) (Entekhabi et al., 2010) satellites.

The depth of soil sensed by these space-borne sensors is dependent on the wavelength of the emitted or reflected microwaves. Consequently, L-band observations correspond to a deeper layer of soil ($\approx$ 3–5 cm) compared to shorter wavelengths such as X- and C-band ($\approx$ 1–2 cm), and are less affected by the overlying layer of vegetation (Naeimi et al., 2009). This makes L-band the theoretically more optimal frequency for soil moisture estimation (Escorihuela et al., 2010; Kerr et al., 2012). In addition to frequency choice, microwave sensors can also operate as an active or passive system. Nevertheless, this study concentrates on the latter due to the reduced effects of surface roughness on vegetation signal interpretation.

Microwave emission from the land surface, commonly referred to as brightness temperature, is proportional to the product of effective temperature from the emitting layer and surface emissivity (Schmugge et al., 2002). Measurements of brightness temperature from space-borne sensors are converted into soil moisture products through radiative transfer models (e.g. Mo et al., 1982; Njoku and Li, 1999; Owe et al., 2001; Wen and Su, 2003). Consequently, the accuracy of these products are not only prone to errors from the sensors themselves, including the frequency of observation, but also the parameters and assumptions applied in these models. Moreover, satellite missions such as AMSR2 and SMOS have defined a specific set of performance requirements. In the case of AMSR2 soil moisture products, the performance requirement is defined as the mean absolute error (MAE) of instantaneous observations with the research product (Level 3; 25 km) having a *goal accuracy* of $< \pm 0.08$ m^3/m^3 (JAXA, n.d.; Maeda et al., 2011). For SMOS, the goal is a maximum root mean square error (RMSE) < 0.04 m^3/m^3 in the top 5 cm soil layers without accounting for long-term bias correction (Kerr et al., 2010). However, the evaluation of these soil moisture products is complicated by errors in both data sets and differences between the horizontal (spatial) and vertical (depth) scales detected by remotely sensed and ground-based soil moisture (e.g. Crow et al., 2012). Still, evaluation of remote sensing soil moisture products has often been based on arbitrarily selected stations or the average of stations which fall within the satellite pixel (e.g Albergel et al., 2012; Brocca et al., 2012; Cho et al., 2015; Choi, 2012; Dente et al., 2012b; Draper et al., 2009; Jackson et al., 2012; Kim et al., 2015; Su et al., 2013; Wu et al., 2015), and by assuming these measurements are representative of the satellite's sensor resolution.

In some studies, *in situ* measurements have been up-scaled based on geostatistical methods such as block-kriging or triangulation interpolation methods, or even land surface model simulations (e.g. Brocca et al., 2011; Dall'Amico et al., 2012; Rötzer et al., 2014). The downside of depending on a number of stations is that measurements are not always available from all sites. To overcome this, Su et al. (2013) and van der Schalie et al. (2015) employed a lookup method whereby the stations were ranked according to their representativeness of the mean area average. Yet, this leads to an inconsistency in the quality of measurements used for evaluation. Moreover, the uncertainties in land surface model simulations may emanate from inaccuracies in input forcing used to drive the models, parameters prescribed within the model physics, and structural errors within the physical equations of the models (Crow et al., 2005; Seneviratne, 2010; Zhang et al., 2013).

To address the issue of non-representativeness, and demonstrate the impact of poorly selected stations, evaluation of remote sensing soil moisture products herein is based on the careful selection of stations from an earlier study of Yee et al. (2016) using a combination of geostatistical analysis of intensive soil moisture measurements and temporal stability analysis of long-term soil moisture stations. These most representative stations have been used to evaluate soil moisture products from AMSR2 and SMOS, with the AMSR2 products derived from two different algorithms, i.e. the algorithm developed by Japan Aerospace eXploration Agency (JAXA) and the Land Parameter Retrieval Model (LPRM). Of the JAXA algorithm, two different versions were compared, and of the LPRM algorithm, three versions. Whilst previous studies have evaluated the AMSR2 soil moisture products (e.g. Kim et al., 2015; Wu et al., 2015), a calibration misalignment between AMSR-E and AMSR2 led to reprocessed products from the JAXA (JAXA, 2015) and LPRM algorithms (Parinussa et al., 2015). This necessitates a comparison between the different versions from each algorithm. Further development of the LPRM parameterization scheme following van der Schalie et al. (2015) also led to the production of another version of AMSR2 LPRM product which has yet to be evaluated. Moreover, products have been derived based on the LPRM algorithm for observations at C-band (6.9 GHz and 7.3 GHz, hereon denoted as C1 and C2 respectively) in addition to X-band (10.7 GHz, hereon denoted as X).

The occurrence of radio frequency interference (RFI) at C-band has often prevented the use of C-band observations in North America, Middle East and Japan (Njoku et al., 2005). Similarly, RFI at X-band has been detected in Italy and Great Britain (e.g. Lacava et al., 2012), and at L-band in Europe, China and Canada. However, as Australia has been found to be largely unaffected by RFI, an opportunity to compare products from these different frequencies presents itself. The inclusion of two versions of SMOS products extends the comparison of wavelengths to L-band (1.4 GHz) and highlights the impact of using stations of poor choice. Consequently, this comprehensive comparison of different soil moisture products affords 1) an understanding of how well each product meets its respective performance requirements under tightly controlled analysis, and 2) identification of the best performing product under the conditions of this site.

2. Data and methods

2.1. Study area and in situ soil moisture data

This evaluation study was carried out for the Yanco site, which is within the Murrumbidgee River catchment in New South Wales, Australia (Fig. 1). The area has been extensively monitored for remote sensing research through a soil moisture monitoring network (Oznet; Smith et al., 2012) and a series of field experiments for the pre- and post-launch algorithm development of missions such as SMOS and SMAP; National Airborne Field Experiment 2006 (Merlin et al., 2008), Australian Airborne cal/val Experiments for SMOS (Peischl et al., 2012) and Soil Moisture Active Passive Experiments (SMAPEx) (Panciera et al., 2014). Generally, the Yanco area is flat with elevations ranging from 117 m to 150 m. Based on soil texture analysis at the site, the top layer soil of the region is predominantly silty loam, loamy sand, sand loams (McKenzie et al., 2000). Mean daytime temperature of the region falls between 32°C in January and 13°C in July, with a mean annual rainfall of 418 mm which is well-distributed throughout the year (Bureau of Meteorology station ID. 074037).

The western side of the study area includes the Coleambally Irrigation Area (CIA), which consists of farms with a mix of flood irrigation and dryland cropping. Main crops grown during summer include rice, corn, and soybeans, whereas wheat, oat, barley and canola are grown during winter. Flood irrigation of rice crops occurs in November (Panciera et al., 2014). Conversely, land use to the eastern side of the site consists of pastures for grazing. To differentiate these two areas, YA is used to describe the cropping area, and YB for the grazing area. There are 13 profile soil moisture stations within the study area (denoted with the prefix 'Y-') equipped with vertically installed Stevens Water Hydraprobe (0–5 cm) and Campbell Scientific CS616

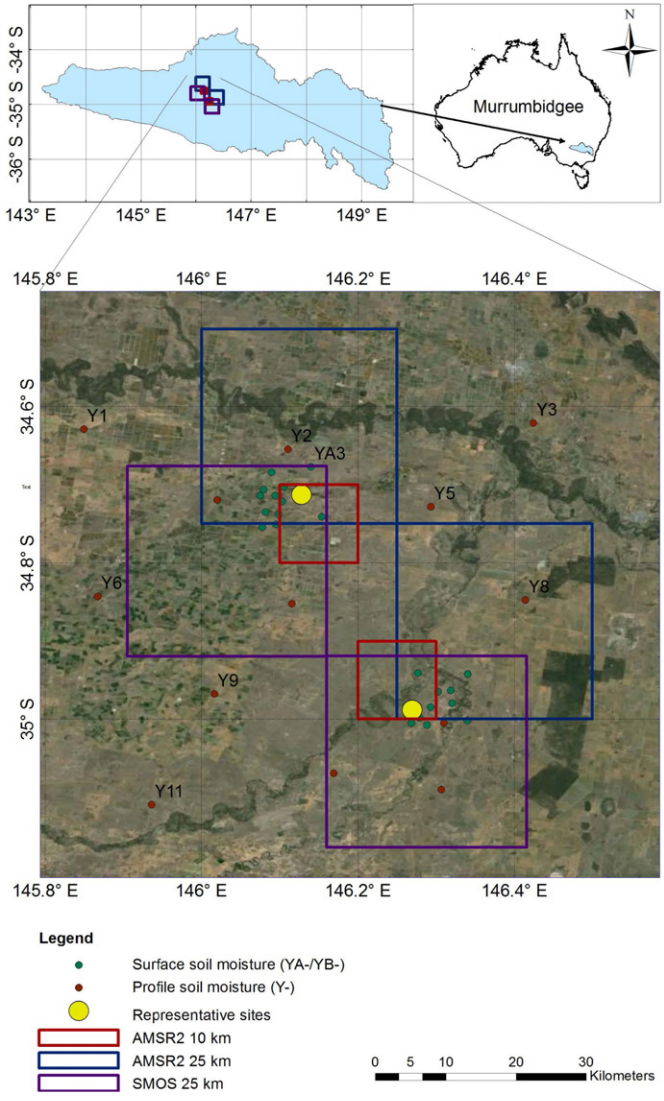

Fig. 1. Map of study area showing locations of soil moisture monitoring stations and the most representative stations, together with satellite pixels selected for evaluation. The top left inset shows the relative location of the study area within the Murrumbidgee catchment.

water reflectometers (0–30 cm, 30–60 cm, and 60–90 cm); and 24 surface soil moisture stations equipped with a Hydraprobe inserted vertically from the surface (0–5 cm) concentrated within the YA and YB areas (denoted 'YA-' and 'YB-' in Fig. 1). To compare as closely as possible with the depth sensed by the microwave sensors, only measurements from 0 to 5 cm have been used herein (Adams et al., 2015). As AMSR2 more correctly represents a 1 cm or so soil layer, it is slightly penalized compared to SMOS, which represents a 3–5 cm soil layer (Table 1).

2.2. Satellite soil moisture data

2.2.1. AMSR2

AMSR2 on-board the GCOM-W1 satellite was launched in May 2012 as a follow-on of AMSR for the EOS (AMSR-E, May 2002 to Oct 2011). Compared with AMSR-E, AMSR2 has a larger antenna (2.0 m diameter) than AMSR-E (1.6 m diameter), an additional C-band (7.3 GHz) channel to mitigate RFI (e.g. de Nijs et al., 2015), and an improvement in calibration accuracy through a change in thermal design (Imaoka et al., 2010; Maeda et al., 2011). Observations from AMSR2 are available twice daily (ascending/evening and descending/morning) every one to two days.

The AMSR2 products compared herein are based on the JAXA (Fujii et al., 2009; Maeda and Taniguchi, 2013) and LPRM (Owe et al., 2001; Parinussa et al., 2015) algorithms. Due to an improvement in calibration of brightness temperatures from AMSR2, both JAXA and LPRM products have been reprocessed. The JAXA AMSR2 Level 3 soil moisture content data products, version 1.11 (herein referred to as JX1) and version 2.21 (herein referred to as JX2), were obtained from the GCOM-W1 Data Providing Service (https://gcom-w1.jaxa.jp/). As JX1 was only available until the end of 2014; and to obtain an equal number of seasons, soil moisture products from July 2012 to July 2014 were considered herein. This study differs from the evaluation study carried out by Wu et al. (2015) over the United States in that they did not differentiate the two product versions, and Zeng et al. (2015) which only used JX1. As for the LPRM products, the product based on the former brightness temperatures (herein referred to as LP1) was obtained from Goddard Earth Sciences Data and Information Services Center (GES DISC) (http://disc.sci.gsfc.nasa.gov/hydrology/), whereas the updated version (herein referred to as LP2) was reprocessed following Parinussa et al. (2015). In addition, a third version of the LPRM product (LP3) was also included in this analysis. The difference between LP2 and LP3 is that LP3 was derived based on the recalibrated brightness temperatures of AMSR2, and a new parameterization scheme following van der Schalie et al. (2015). In LP2, the single scattering albedo was based on a best guess whereas that of LP3 was calibrated through in-situ measurements together with a vegetation correction. The AMSR2 products are available at 10 km and 25 km grid resolutions although its footprint is approximately 50 km. Hence, products of 10 km and 25 km were included in the analysis for both evening (1:30 pm) and morning (1:30 am) overpasses (Table 2).

2.2.2. SMOS

Launched in 2009, the radiometer aboard SMOS measures L-band emissions at 1.4 GHz every 3 days. While the resolution of SMOS is approximately 40 km (Kerr et al., 2001), the soil moisture L3 products are provided on a 25 km grid resolution. These products are derived based on the SMOS L2 Processor, which is based on the L-band microwave emission of the biosphere (L-MEB) model. The model involves an iterative algorithm to minimize a cost function computed from the differences between measured and modelled brightness temperature from all available incidence angles (Wigneron et al., 2007). In this case, the data used was obtained from the Centre Aval de Traitement des Données SMOS (CATDS), operated by the Centre National d'Etudes Spatiales (CNES, France) by IFREMER (Brest, France) (Jacquette et al., 2010). The daily 25 km grid resolution SMOS Level 3 products including both ascending/morning (6:00 am) and descending/evening (6:00 pm) overpasses of two different versions were used. The SMOS products compared were the CATDS version 2.72 product (SMOS1) and version 3.00 products (SMOS2). As reprocessed soil moisture products from SMOS1 (EASE grid) were only available for 2012 to 2013, the operational product was used for 2014 (EASE2 grid). SMOS2 reprocessed products were available from July 2012 to July 2014 and are on the EASE2 grid. For consistency, it is assumed herein that all products are on the EASE2 grid. Within the study area, this change in grid version is negligible. Instances when the probability of RFI was flagged as higher than 0.05 were also removed.

To differentiate the products, AMSR2 and SMOS products have assigned subscripts denoting the observed frequency used (X, C1 or C2), the overpass (M: morning/AM, E: evening/PM), and product resolution (10 or 25), whereas superscripts denote the area being evaluated (YA or YB). For instance, $JX1^{YA}_{X(M),25}$ is the 25 km soil moisture product based on the JAXA algorithm (version 1), derived from observations at X-band during morning overpasses at the YA area.

Table 1
Overview of passive microwave soil moisture satellites used in this study.

Spacecraft	SMOS	GCOM-W1
Sensor	Microwave Imaging Radiometer using Aperture Synthesis (MIRAS)	The Advanced Microwave Scanning Radiometer 2 (AMSR2)
Swath width	1000 km	1445 km
Sensor accuracies	1.8 K (at 180 K)	0.66 K (at 100 K)
	2.2 K (at 220 K)	0.68 K (at 250 K)
Frequency	1.41 GHz (L-band)	6.9, 7.3 and 10.7 GHz (C-band and X-band)
Footprint dimensions (km^2)	43 km on average over the circle field of view	24–35 km × 42–62 km ellipse
Sampling interval (km)	≈ 15	≈ 10
Product posting (km)	≈ 25	≈ 10/≈ 25
Temporal resolution	2–3 days	1–2 days
Launch date	2nd Nov. 2009	18th May 2012
Target accuracy	RMSE < 0.04 m^3 m^{-3}	MAE < 0.08 m^3 m^{-3}
Node	Ascending Descending	Descending Ascending
Equator crossing	6:00 AM 6:00 PM	1:30 AM 1:30 PM
M/E	Morning Evening	Morning Evening

2.3. Analysis

Based on results in Yee et al. (2016), incorrect conclusions and biases may have been introduced into the results of earlier studies that did not have a good understanding of the sites. Therefore, coarse scale passive microwave remote sensing soil moisture products are evaluated herein based on a careful understanding of the representativeness of stations within the YA and YB areas. These stations were identified in the aforementioned study based on geostatistical analysis of intensive soil moisture measurements taken from field campaigns at the study area, and temporal stability analysis of long-term soil moisture measurements from stations within the OzNet network. Since stations within the Yanco area are well-distributed, based on temporal stability methods, YA5 and YB7a were found to provide a good measure of the areal average of the YA and YB area (≈ 9 km × 9 km), and YA5 for the Yanco region (≈ 36 km × 36 km) (Fig. 1). It is assumed herein that although results from the previous analysis focused on SMAP grids, they are transferable to the AMSR2 and SMOS 25 km grids due to relatively high homogeneity of the site. As the native footprint of the satellites overlaps the adjacent pixels, measurements from other stations around the pixels were also used to compute an average for the entire pixel. Pixels with center points closest to the YA and YB focus areas were selected for evaluation (Fig. 1) and are summarized in Table 3.

Consistent with mission objectives, the statistical metrics that are used to evaluate the products include bias, root mean square difference (RMSD) (similar to RMSE), Pearson correlation coefficient (r), MAE and unbiased RMSD (ubRMSD). Bias was computed as the difference between remotely sensed soil moisture in relation to ground measurements. MAE is the average of the absolute errors, and differs from RMSD in that the squaring of the errors in RMSD gives a greater weight to larger errors.

Taylor diagrams are used to combine measures of r, standardized centered RMSD (cRMSD) and standardized standard deviation with ground soil moisture measurements (Taylor, 2001). Taylor diagram provides a comprehensive visualization of how well two datasets relate to each other in terms of r, RMSD and their standard deviations. They have also recently been applied for soil moisture evaluation by Champagne et al. (2015). The geometric relationship between these statistics allows the Taylor diagram to be plotted. For N discrete points of two variables, f_n and g_n, r is given as

$$r = \frac{1}{\sigma_f \sigma_g} \sum_{N}^{n=1} (f_n - \bar{f})(g_n - \bar{g}), \tag{1}$$

where $\bar{f}$ and $\bar{g}$ are their means, and σ_f and σ_g are the standard deviations, of f and g respectively. The cRMSD, which is the ubRMSD, is then given by

$$\mathrm{cRMSD} = \sqrt{\frac{1}{N} \sum_{N}^{n=1} \left[(f_n - \bar{f})(g_n - \bar{g}) \right]^2}. \tag{2}$$

The maximum soil moisture established in the JAXA algorithm is 0.60 m^3/m^3 whereas for the LPRM algorithm is 1.00 m^3/m^3 (Kim et al., 2015). Therefore, assuming f_g is the reference dataset, these statistics were further standardized by σ_g such that standardized cRMSD, $\widehat{\mathrm{cRMSD}} = \mathrm{cRMSD}/\sigma_g$, and standardized σ_f, $\widehat{\sigma}_f = \sigma_f/\sigma_g$ (Albergel et al., 2012). Consequently, $\widehat{\sigma}_g = 1$. Note that although this procedure was referred to as normalization in Taylor (2001), the term standardization is used herein. Therefore, the radial distance of f_n from the origin represents $\widehat{\sigma}_f$, the radial distance from the reference represents $\widehat{\mathrm{cRMSD}}$, and finally, the azimuthal position represents r between f_g and f_n. A more comprehensive description regarding the derivation and use of the Taylor diagram can be found in Taylor (2001).

As the general consensus within the remote sensing community is that morning observations are more ideal than those later in the day (referred to as evening herein), due to the difference in temperature between vegetation canopy and soil surface being at a minimum, the analysis herein will firstly concentrate on morning observations and 25 km products. Comparisons with evening observations and 10 km products will be introduced in later sections of this paper.

Table 2
Summary differences between validated products.

Spacecraft	Acronym	Version update/change
AMSR2	JX1	Version 1.11 based on JAXA algorithm (Fujii et al., 2009; Maeda et al., 2011) without correction of calibration misalignment between AMSR-E and AMSR-2.
	JX2	Version 2.21 based on JAXA algorithm using recalibrated brightness temperature calibration.
	LP1	Derived using LPRM algorithm with former brightness temperatures. Obtained from Goddard Earth Sciences Data and Information Services Center (Owe et al., 2001).
	LP2	Reprocessed LPRM products using calibrated brightness temperature. Single scattering albedo based on a best guess (Parinussa et al., 2015).
	LP3	Reprocessed LPRM products using calibrated brightness temperature. Single scattering albedo calibrated through in-situ measurements together with a vegetation correction (van der Schalie et al., 2015).
SMOS	SMOS1	CATDS algorithm (Jacquette et al., 2010) version 2.72 based on EASE1 grid.
	SMOS2	CATDS version 3.00 based on EASE2 grid.

Table 3
Pixel centre of soil moisture products, and corresponding stations selected for this validation study.

	Grid resolution	Pixel centre		Focus area		
Product	(km)	Lat	Lon	YA/YB	Stations	Rep. station
AMSR2	25	−34.63	146.13	YA	Y2, Y4, Y7, YA1, YA3, YA4a,	YA5
AMSR2	10	−34.75	146.15	YA	YA4b, YA4c, YA4d, YA4e, YA5,	
SMOS	25	−34.70	146.15	YA	YA7a, YA7b, YA7d, YA7e, YA9	
AMSR2	25	−34.75	146.38	YB	Y10, Y12, Y13, YB1, YB3, YB5a,	YB7a
AMSR2	10	−34.95	146.25	YB	YB5b, YB5e, YB7a, YB7b/YB5d,	
SMOS	25	−34.93	146.41	YB	YB7c, YB7d, YB7e, YB9	

3. Results and discussion

3.1. Representativeness

To contrast results when random stations or representative stations are used, Figs. 2 and 3 summarize the statistics from comparison of individual stations with selected satellite soil moisture products for each season (Summer: December–February; Autumn: March–May; Winter: June–August; Spring: September–November) within the YA and YB area respectively as Taylor diagrams. The same comparisons for the remaining products are provided in the Appendix. The squares indicate the representative stations, diamonds the average based on all stations, and circles all other individual stations. Generally, the closer a point is to the baseline (black point), the better its performance.

The scatter of circles within the Taylor diagrams for the YA area (Fig. 2), particularly during summer and winter, indicates that statistics differ significantly depending on the stations used for evaluation. Some individual stations were found to have an r of < 0.1 (stations with $r < 0$ are not shown) or a $\widetilde{\text{cRMSD}} > 1.5$ m^3/m^3. Further investigation (not shown herein) revealed that during summer and autumn, YA4b and YA4d recorded high soil moisture values (> 0.40 m^3/m^3) due to irrigation. Individually, using SMOS2 25 km grid resolution soil moisture products (morning overpasses) as a reference, comparison against stations YA4b and YA4d had an overall r of 0.03 and −0.34, RMSD of 0.17 m^3/m^3 and 0.28 m^3/m^3, and bias of −0.11 m^3/m^3 and −0.20 m^3/m^3 respectively. Other stations had an r ranging between 0.27 and 0.82, RMSD between 0.05 m^3/m^3 and 0.11 m^3/m^3, and bias between 0.01 m^3/m^3 and 0.10 m^3/m^3. Although these irrigated plots consist only of approximately 0.10% of the entire 25 km pixel, they can have a substantial impact on the average soil moisture if not weighted appropriately (Yee et al., 2016).

In the case of the YB area, the scatter in data points (Fig. 3) is seen to be less apparent due to homogeneity of the area. In comparison

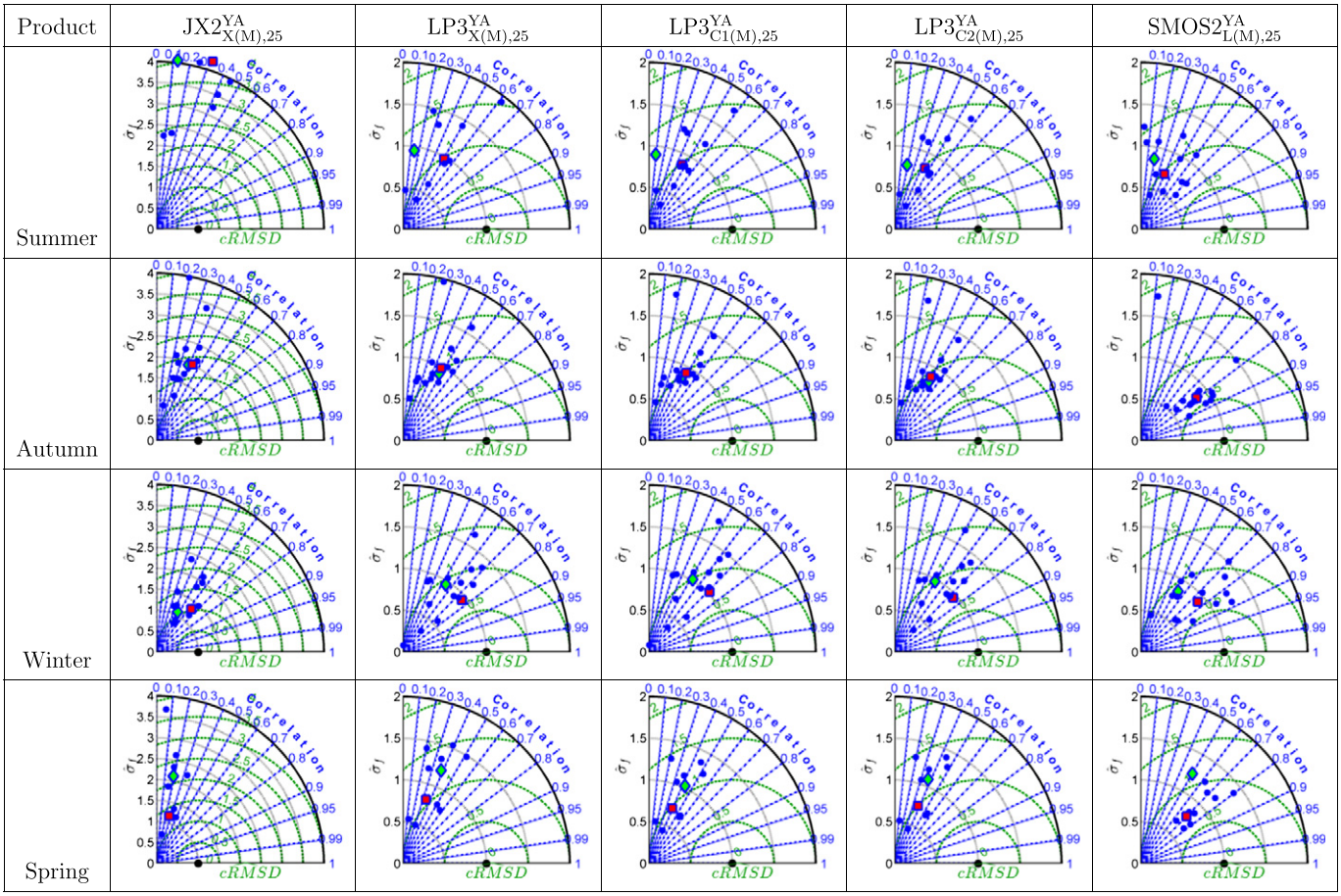

Fig. 2. Taylor diagrams for 25 km grid resolution morning products in the YA area. Satellite products are treated as the baseline soil moisture (black dot). □: Representative station. ⋄ : Average. ◯: Individual stations. Note the difference in scale for JAXA products.

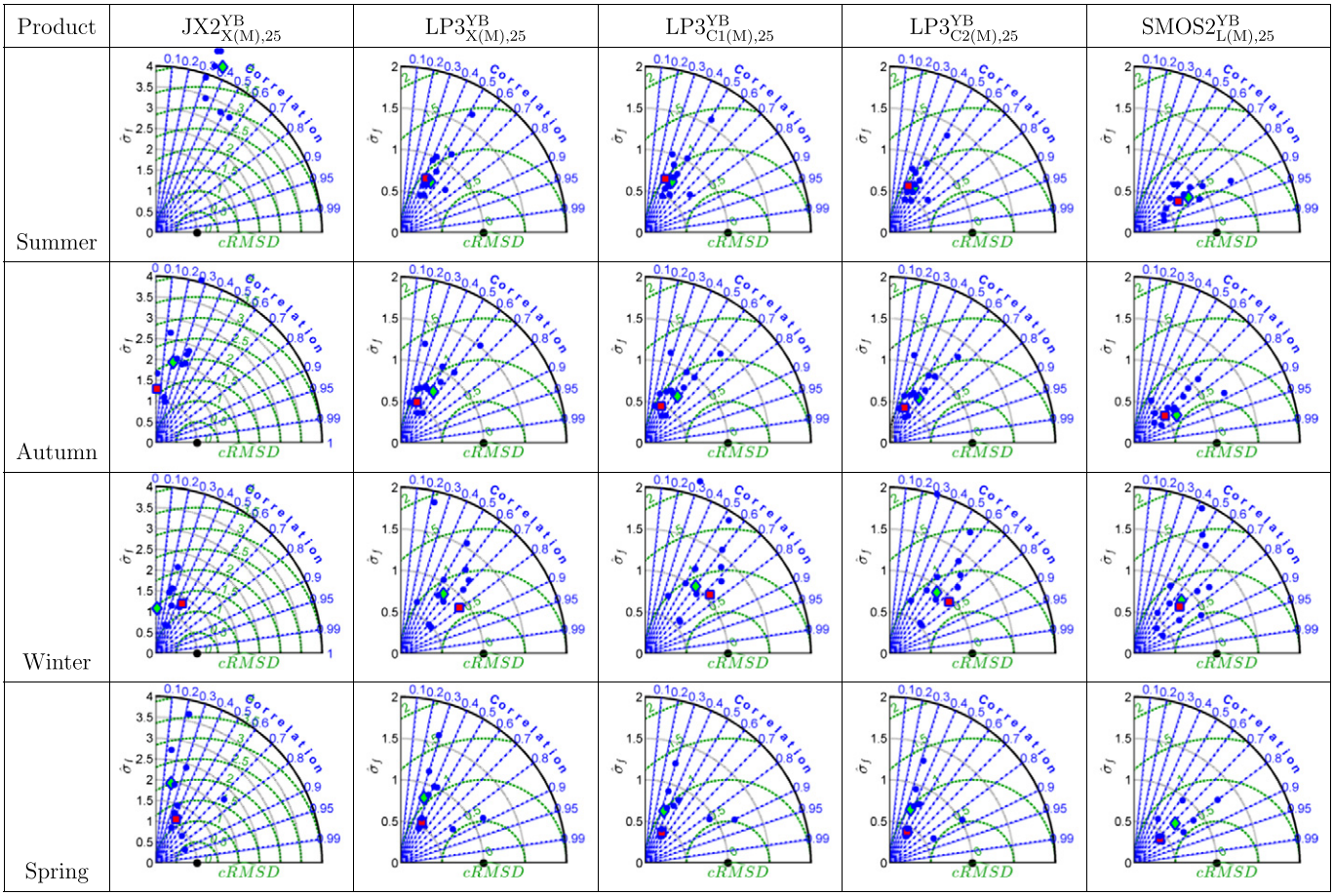

Fig. 3. Taylor diagrams for 25 km grid resolution morning products in the YB area. Satellite products are treated as the baseline soil moisture (black dot). □: Representative station. ⋄: Average. ◯: Individual stations. Note the difference in scale for JAXA products.

to the SMOS2 25 km grid resolution soil moisture products (morning overpasses), r ranged between 0.37 and 0.90, RMSD 0.05 m^3/m^3 and 0.11 m^3/m^3, and bias between 0 m^3/m^3 and 0.08 m^3/m^3. The red and green circles consistently give amongst the best results, and r and RMSD between the average of all stations and the representative stations yielded similar results (as identification of the representative station was in large based on its ability to represent the mean). Conversely, a big variation can be found if a single station was used without prior knowledge of its representativeness. This also demonstrates that, whilst the absolute accuracy of a representative station is difficult to determine, by directing limited resources to most representative sites, similar results can be obtained as having a number of stations. Results herein have shown the importance of understanding the representativeness of soil moisture stations prior to using them for evaluation. Consequently, the satellite soil moisture products will be evaluated based on the representative stations YA5 and YB7a for the YA and YB area respectively which were determined based on SMAP grids (Yee et al., 2016) for the remainder of this paper.

3.2. Overall performance

Based on comparison with the representative stations, there is a noticeable seasonal impact on the performance of absolute soil moisture based on JX2 whereby $\widehat{cRMSD}$ decreased sequentially from summer, autumn, spring and winter (Figs. 2 and 3). This was more consistent for the LPRM and SMOS products, where $\widehat{cRMSD}$ was ≈ 1 throughout the year. The JAXA algorithm assumes that surface and canopy temperature is both equal and constant throughout the year at 295 K. Whilst canopy temperatures are not compared herein, it is expected that this assumption would be valid only during winter. Consequently, $\widehat{cRMSD}$ is lowest during winter and highest during summer.

When compared with measurements from YA5 and YB7a, JX1 and JX2 underestimated soil moisture by < 0.06 m^3/m^3 and had an r of approximately 0.5, while LPRM products overestimated (ranging from 0.04 m^3/m^3 to 0.23 m^3/m^3), particularly when soil moisture conditions were > 0.10 m^3/m^3 (Fig. 4 and 5). Moreover, it can be seen that performance of the JAXA algorithm decreased with increasing soil moisture values, whereas the opposite is true for LPRM. Kim et al. (2015) found similar results when comparing AMSR2 soil moisture products based on the JAXA and LPRM algorithm globally. Furthermore, only a slight improvement was observed in the JX2 version of the JAXA products with a reduction of MAE from 0.06 m^3/m^3 to 0.05 m^3/m^3 and a slight increase of r.

In the case of LPRM products, while LP1 had a larger RMSD (0.13–0.26 m^3/m^3) and MAE (0.10–0.23 m^3/m^3) than JX1 and JX2, a substantial improvement was found in LPRM products based on the recalibrated brightness temperatures, i.e. LP2 whereby RMSD and MAE decreased to 0.06–0.11 m^3/m^3 and 0.07–0.13 m^3/m^3 respectively. Generally, this improvement was most pronounced for observations at 7.3 GHz followed by 6.9 GHz whereby correlation increased to > 0.55 for both but did not change much for X-band observations (Fig. 4 and 5). Further improvements were found with C-band LP3 products that utilized the new parameterization method whereby correlation was found to increase by 0.05 at the YA area and 0.07 at the YB area. At X-band, the improvements were more modest at 0.01 and 0.03 at the YA and YB area respectively. Moreover, whilst RMSD and MAE decreased for LP3 products at C-band, they increased

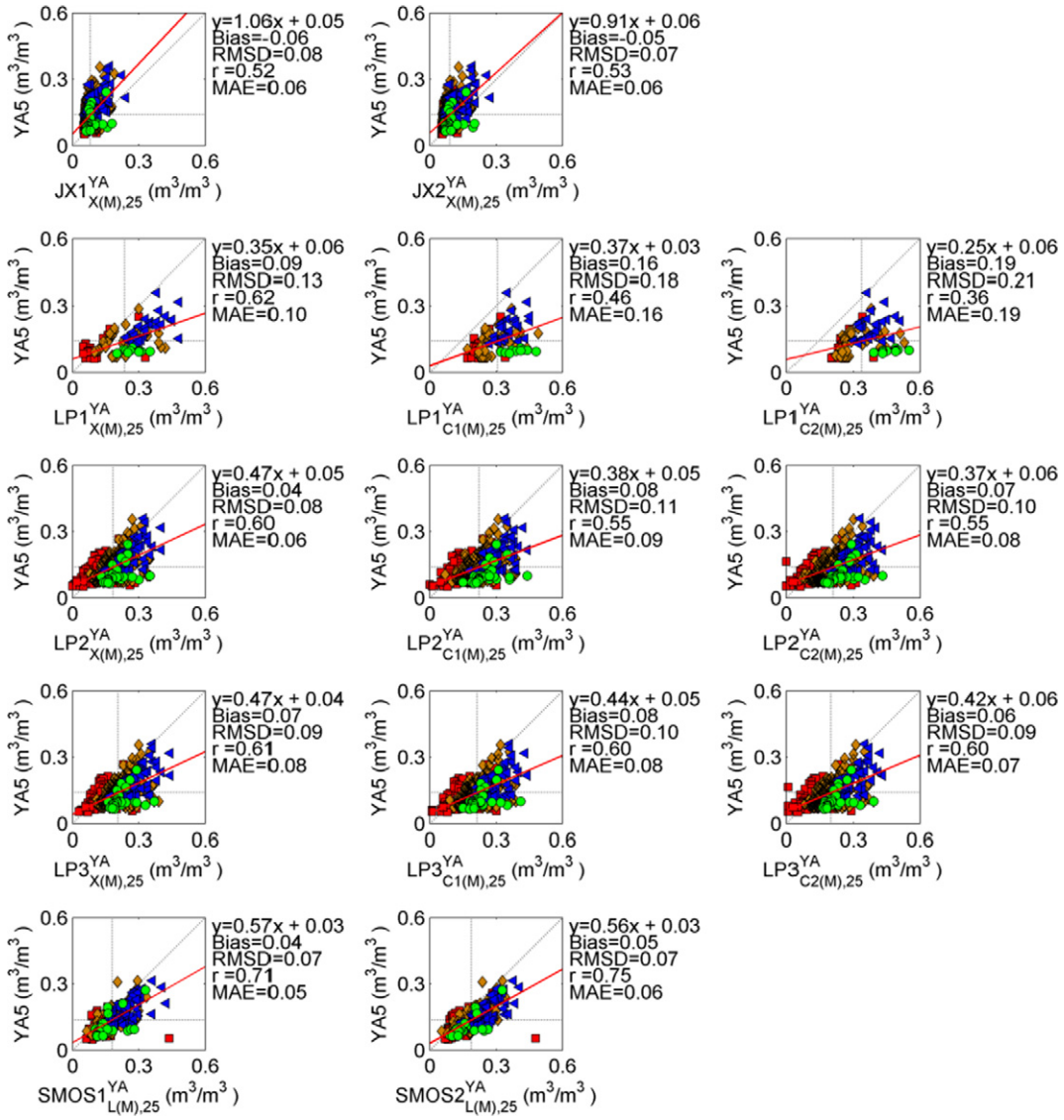

Fig. 4. Scatterplots comparing different morning overpass soil moisture products in the YA area with the most representative station YA5 as the baseline. Summer: □ (Red), Autumn: ⋄ (Orange), Winter: ◁ (Blue), Spring: ○ (Green). Dotted horizontal and vertical lines indicate the means of the corresponding x- or y-axis variables, whereas the diagonal line is the 1:1 line.

slightly at X-band. Nevertheless, the suit of LP3 products were found to be superior over its predecessors with products based on 10.7 GHz performing the best, followed by 7.3 GHz and 6.9 GHz.

Finally, SMOS products performed better than AMSR2 products with an r > 0.71 and a bias of < 0.05 m^3/m^3 for both versions. The scatter along the fitted line is also well-distributed (Fig. 4 and 5). Generally, the SMOS products slightly underestimate, agreeing with the findings of previous studies (Al Bitar et al., 2012; Collow et al., 2012; Su et al., 2013). Comparing SMOS1 and SMOS2, SMOS2 performed better due to a 0.04 increase in r, whereas accuracy in absolute soil moisture was similar in both versions. As the latter products based on the JAXA, LPRM and SMOS algorithm were found to be superior over the former versions, only JX2, LP3 ('X-' and C-band) and SMOS2 are discussed in detail in the following analyses.

3.3. Performance for different overpass periods, frequencies and resolutions

The large variation in soil moisture measurements based on individual stations (grey lines) in Fig. 6 re-emphasizes the need for evaluation with most representative stations. Generally, it can be seen that soil moisture retrieved based on JX2 was the driest followed by SMOS2, $LP3_X$, $LP2_{C2}$ and $LP2_{C1}$ for both morning and evening overpasses. The variation in soil moisture was also observed to be lower during evening overpasses. There was a clear underestimation by JX2 with a more noticeable difference in morning retrievals rather than evening when NDVI was high (Fig. 6). Moreover, as LP3 and SMOS2 did not display this pattern, the underestimation is most likely due to the algorithm as observed earlier.

Both JX1 and JX2 showed the lowest variations whereby $\hat{\sigma}_{JX1}$ and $\hat{\sigma}_{JX2}$ ranged between 0.5 and 1 (Fig. 7). Correspondingly, this led to the underestimation observed earlier and its $\widehat{cRMSD}$ being the lowest in all cases. Despite this, accounting for r, RMSD and standard deviation, the JAXA products were found to be closest to the baseline measurements (black dot) in the YA and YB area, for morning and evening overpasses, and for both 25 km and 10 km resolutions.

It was also found that evening overpass (1:30 pm) products performed better for both the JAXA and LPRM algorithm than the

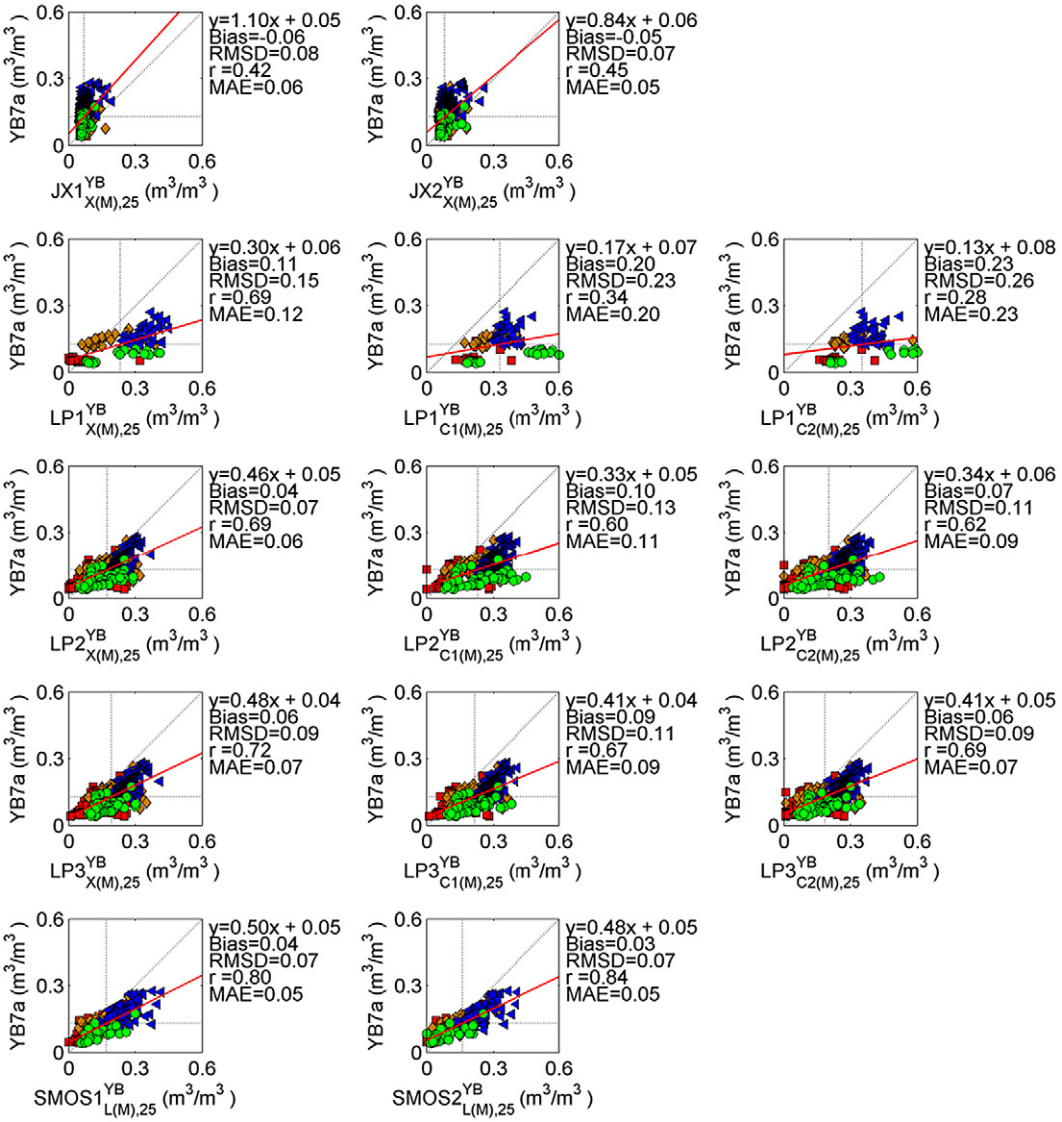

Fig. 5. As for Fig. 4 except YB area with the most representative station YB7a as baseline.

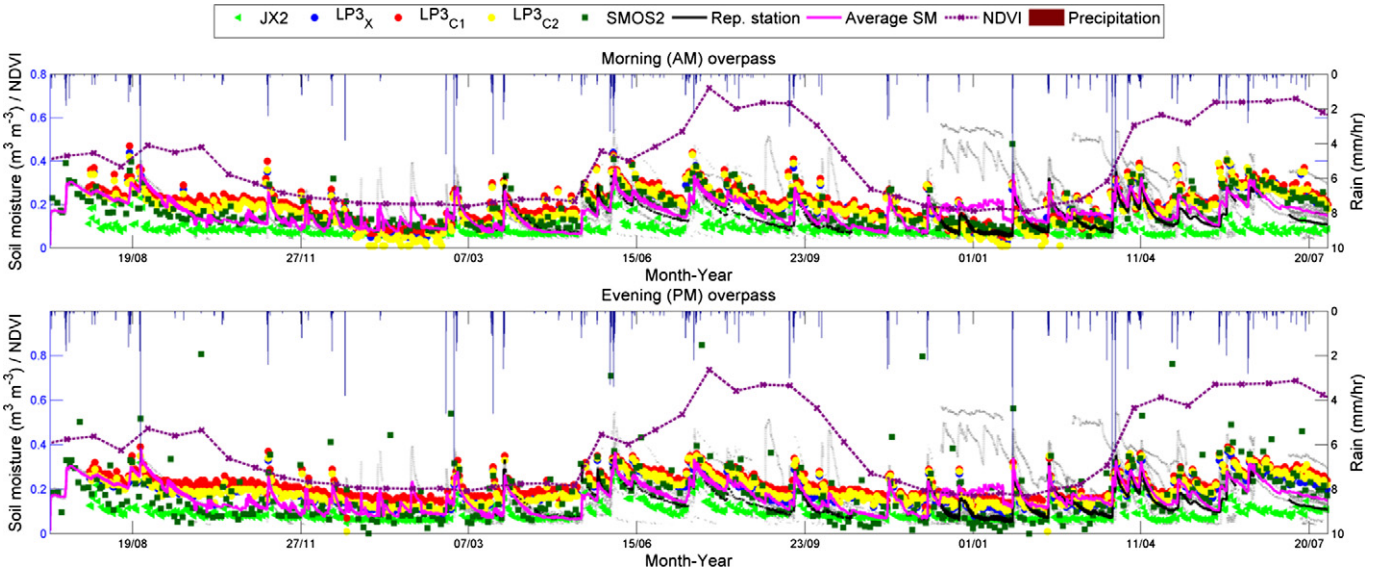

Fig. 6. Timeseries of morning (top) and evening (bottom) observations for the different 25km grid resolution satellite products, most representative station and station average, MODIS NDVI and site precipitation from July 2012 to July 2014 for the YA area.

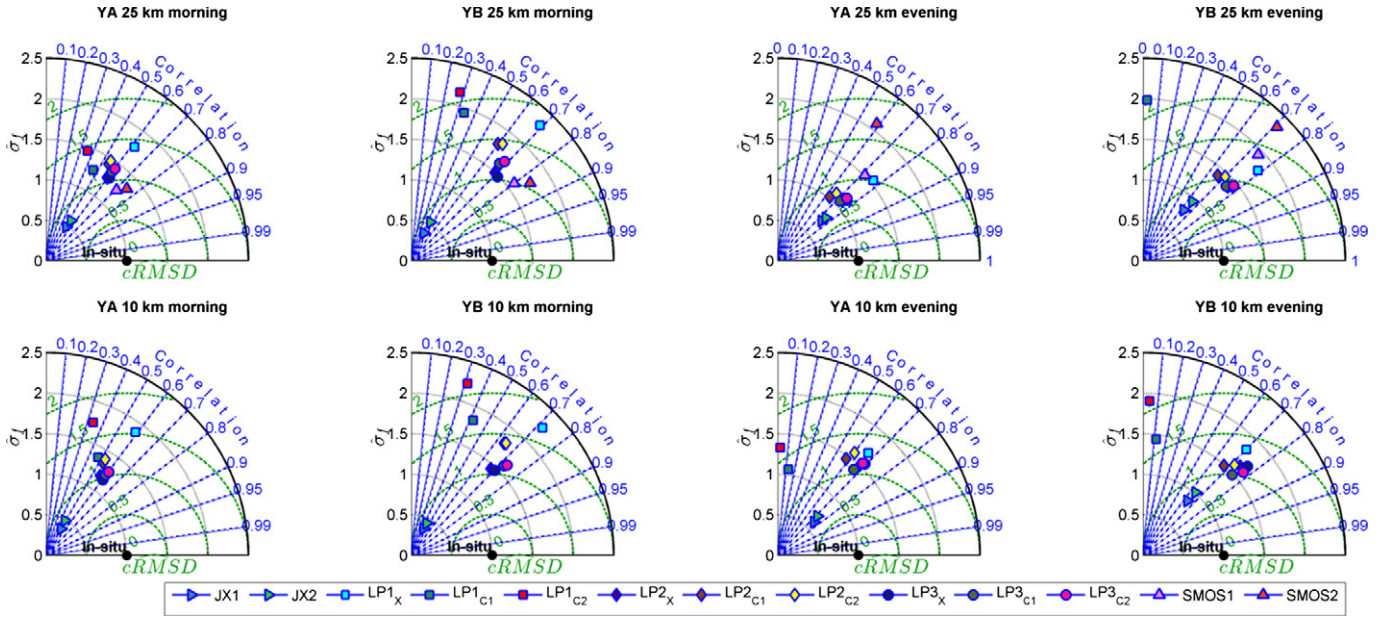

Fig. 7. Taylor diagrams comparing 25km (top) and 10km (bottom) grid resolution morning and evening products for the YA and YB area. Note: SMOS products are not available on a 10km resolution grid.

morning passes (1:30 am). With the exception of $LP1_{C1}$ and $LP1_{C2}$ which were not shown on the diagrams due to the negative r, the variation of soil moisture based on the evening overpasses matched better with that of the stations ($\hat{\sigma}_f$ closer to 1) than morning overpasses. LP1 C-band observations were previously found to perform badly due to model miscalibration which was rectified in LP2 and therefore should not be used (Parinussa et al., 2015). Conversely, whilst morning overpasses from SMOS1 and SMOS2 were found to perform well during the morning overpasses, SMOS2 evening overpasses overestimated the soil moisture ($\hat{\sigma}_f > 1.5$) and were less accurate compared with the AMSR2 products. Previous evaluation studies regarding morning and evening observations have yielded mixed results for both AMSR-E/-2 (e.g. Brocca et al., 2011; Draper et al., 2009; Griesfeller et al., 2015) and SMOS (e.g. Dente et al., 2012a; Djamai et al., 2015; Rowlandson et al., 2012). Du et al. (2012) and Raju et al. (1995) stipulated issues in inverse modelling of soil moisture at night or early morning for frequencies higher than 5.05 GHz when dry soil is slightly wetted as a consequence of dew or early stages of rainfall. This effect should be less on L-band observations which senses a deeper layer. Other factors such as difference in temperatures between near surface soil and vegetation can also affect the accuracy of the retrievals at different times of day (Entekhabi et al., 2010; Kerr et al., 2010). A combination of these different factors may have led to the mixed results for AMSR2 retrievals and a more in-depth study will be needed to verify the cause.

In the case of LPRM products, one would expect retrievals based on observations at 6.9 GHz (C1) to correlate better with the 5 cm soil moisture measurements since the depth sensed at lower frequencies should correspond more closely with the 5 cm depth of soil moisture probes and be less affected by the vegetation. However, results showed 10.7 GHz performed better than 6.9 GHz, which overestimated and had a larger variance compared with the station measurements (Fig. 7). Retrievals based on 6.9 GHz and 7.3 GHz were very similar, with 6.9 GHz performing slightly better than 7.3 GHz. This is consistent with the findings of Owe et al. (2008) and Draper et al. (2009) who found few differences between X- and C-band retrievals in Australia.

Overall, based on the Taylor diagrams, JX2 followed by JX1 had the best agreement with representative stations for both YA and YB areas during both overpasses. Considering only the morning overpasses, performance of SMOS1 and SMOS2 closely resembled that of the JAXA products. During the evening overpasses, the performance of $LP3_X$, $LP3_{C1}$ and $LP3_{C2}$ followed after JX2 and JX1 in decreasing order. Similarly, at 10 km resolution, JX2 followed by JX1 agreed the best for both overpasses, while $LP3_X$ products performed the best among the LPRM products.

Finally, it is to be noted that the ranking of the products' performances depends on the metrics considered in the ranking. For instance, although the JAXA products were superior based on the Taylor diagrams, Figs. 4, 5 and 6 showed otherwise. Table 4 tabulates the bias, RMSD, r and MAE derived from validating 25 km grid resolution products for both morning and evening overpasses at the YA and YB area using measurements from representative stations. Based on these statistics, SMOS2 performed better than SMOS1, and LP3 performed better than JX2. Overall, $SMOS2_{L(M)}$ was superior with an $r > 0.75$ whereas JX2, which was found to perform the best based on Taylor diagrams was clearly outperformed by other products in terms of r (0.53 and 0.45 for YA and YB respectively) with the exception of LP1. As Taylor diagram considers the agreement between the datasets based on a combination of r, RMSD and standard deviations, the cause for a low absolute error in the JAXA products is likely a combination of their lower moisture variation (between 0 and 0.30 m^3/m^3), and the low moisture conditions at the site (also between 0 and 0.30 m^3/m^3 at most times). Nevertheless, compared with the mission objectives of AMSR2 and SMOS, the JAXA, LPRM X-band and SMOS products met the AMSR2 objective of and MAE < 0.08 m^3/m^3 but none of the products met SMOS's mission objective of having an RMSD < 0.04 m^3/m^3. Therefore, depending on the application of the soil moisture product, if both absolute and temporal accuracy is of importance, JX2 products are recommended whereas $LP3_X$ products from evening observations and morning retrievals from SMOS2 products from morning overpasses are recommended if temporal accuracy only is needed.

Table 4
Statistics comparing morning and evening 25km grid resolution satellite products with the most representative stations for YA and YB area.

	Original							Original					
Product	Area	N	Bias m^3/m^3	RMSD m^3/m^3	r	MAE m^3/m^3	ubRMSD m^3/m^3	Area	N	Bias m^3/m^3	RMSD m^3/m^3	r	MAE m^3/m^3	ubRMSD m^3/m^3
$JX1_{X(M)}$	YA	320	-0.06	0.08	0.52	0.06	0.05	YB	319	-0.06	0.08	0.42	0.06	0.05
$JX2_{X(M)}$		320	-0.05	0.07	0.53	0.06	0.05		326	-0.05	0.07	0.45	0.05	0.05
$LP1_{X(M)}$		102	0.09	0.13	0.62	0.10	0.09		101	0.11	0.15	0.68	0.12	0.10
$LP1_{C1(M)}$		102	0.16	0.18	0.46	0.16	0.07		103	0.20	0.23	0.34	0.20	0.11
$LP1_{C2(M)}$		102	0.19	0.21	0.36	0.19	0.09		103	0.23	0.26	0.28	0.23	0.12
$LP2_{X(M)}$		300	0.04	0.08	0.59	0.06	0.07		285	0.05	0.08	0.67	0.06	0.06
$LP2_{C1(M)}$		301	0.08	0.11	0.54	0.09	0.08		290	0.10	0.13	0.59	0.11	0.08
$LP2_{C2(M)}$		299	0.07	0.10	0.55	0.08	0.08		280	0.08	0.11	0.58	0.09	0.08
$LP3_{X(M)}$		302	0.07	0.09	0.61	0.08	0.07		293	0.06	0.09	0.72	0.07	0.06
$LP3_{C1(M)}$		302	0.08	0.10	0.60	0.08	0.07		293	0.09	0.11	0.67	0.09	0.07
$LP3_{C2(M)}$		302	0.06	0.09	0.60	0.07	0.07		293	0.06	0.09	0.69	0.07	0.07
$SMOS1_{L(M)}$		211	0.04	0.07	0.71	0.05	0.05		212	0.04	0.07	0.80	0.05	0.05
$SMOS2_{L(M)}$		213	0.05	0.07	0.75	0.06	0.05		213	0.03	0.07	0.84	0.05	0.06
Average		244	0.06	0.11	0.57	0.09	0.07		239	0.07	0.12	0.59	0.10	0.07
$JX1_{X(E)}$	YA	318	-0.05	0.06	0.75	0.05	0.04	YB	376	-0.04	0.06	0.63	0.04	0.04
$JX2_{X(E)}$		318	-0.05	0.06	0.75	0.05	0.04		383	-0.03	0.05	0.65	0.04	0.04
$LP1_{X(E)}$		100	0.04	0.07	0.77	0.06	0.06		123	0.05	0.08	0.78	0.06	0.06
$LP1_{C1(E)}$		100	0.23	0.25	-0.03	0.23	0.09		125	0.25	0.28	0.03	0.25	0.11
$LP1_{C2(E)}$		100	0.27	0.29	-0.13	0.27	0.11		125	0.29	0.32	-0.03	0.29	0.13
$LP2_{X(E)}$		294	0.03	0.05	0.74	0.04	0.04		357	0.04	0.06	0.75	0.05	0.05
$LP2_{C1(E)}$		294	0.09	0.10	0.64	0.09	0.05		357	0.10	0.11	0.66	0.10	0.05
$LP2_{C2(E)}$		294	0.07	0.08	0.66	0.07	0.05		357	0.08	0.09	0.70	0.08	0.05
$LP3_{X(E)}$		295	0.05	0.07	0.75	0.06	0.04		360	0.06	0.07	0.77	0.06	0.05
$LP3_{C1(E)}$		295	0.08	0.09	0.72	0.08	0.05		360	0.09	0.10	0.75	0.09	0.05
$LP3_{C2(E)}$		295	0.06	0.08	0.74	0.07	0.05		360	0.07	0.08	0.77	0.07	0.05
$SMOS1_{L(E)}$		251	0.02	0.07	0.72	0.05	0.06		294	0.02	0.08	0.74	0.06	0.07
$SMOS2_{L(E)}$		252	0.05	0.11	0.59	0.07	0.10		290	0.02	0.10	0.71	0.07	0.10
Average		247	0.07	0.11	0.59	0.09	0.06		297	0.08	0.11	0.61	0.10	0.06

4. Conclusion

This study evaluated AMSR2 soil moisture products of different versions based on two different algorithms (JAXA and LPRM), and two versions of the SMOS soil moisture product, using the most representative stations identified by an earlier study. It was shown that the use of unrepresentative stations can have a large impact on evaluation results (r of −0.16 as opposed to 0.61) particularly for non-homogeneous areas. Therefore, it is paramount that representativeness of stations be well understood prior to use for any evaluation purposes and that studies which have not done this be dismissed as they only add confusion to product accuracy.

Generally, the latter versions of the JAXA (JX2) and LPRM (LP3) products were confirmed to be superior to the former ones. Furthermore, JAXA products were found to underestimate the soil moisture by ≈ 0.05 m^3/m^3, whereas LPRM products overestimated by between 0.04 and 0.23 m^3/m^3. Performance of soil moisture products during different seasons revealed varying performance of JAXA products, possibly due to assumptions that the difference in temperature between the soil surface and canopy is held constant throughout the year. In the case of LPRM, the poor performance of LP1 C-band observations due to model miscalibration was rectified in LP2. Furthermore, the new parameterization scheme of LP3 also improved retrievals based on C-band observations. However, improvements at X-band were minute.

Comparing the two overpasses, evening retrievals at X-band from AMSR2 performed better than morning retrievals. Conversely, SMOS morning retrievals were better than evening. A comparison of LPRM products from different frequencies showed that X-band retrievals performed better than C-band. Although JX2 (RMSD: 0.06 m^3/m^3; r: 0.70) was found to perform the best based on Taylor diagrams, SMOS2 morning retrievals (RMSD: 0.07 m^3/m^3; r: 0.79), and $LP3_X$ evening retrievals (RMSD: 0.07 m^3/m^3; r: 0.76) performed better based on r only. Overall, JX2, LP3, SMOS1 and SMOS2 met the *goal accuracy* of MAE < 0.08 m^3/m^3 but none of the products achieved SMOS's goal of achieving an RMSD < 0.04 m^3/m^3. SMOS morning products had an RMSD of 0.07 m^3/m^3 whereas its evening products had an RMSD of 0.07 m^3/m^3 to 0.11 m^3/m^3. While this study focuses on two carefully selected pixels, they are typical of much of the cropping and grazing land in southeast Australia. However, they likely not reflect the product accuracy in other landscapes. However, they may likely reflect the product accuracy in other landscapes. Therefore, it is important that such careful analysis can be conducted at other sites.

Acknowledgements

This study was made possible through the provision of OzNet data financially supported by three grants from the Australian Research Council (ARC) (DP140100572, DP0984586). RM Parinussa would also like to acknowledge the support from the ARC grant DP11410102394. MS Yee acknowledges the support from the Australian Postgraduate Award (APA) Scholarship. The authors would like to thank Richard de Jeu for the LP1 dataset made available online through the Goddard Earth Sciences Data and Information Services Center (GES DISC). Similarly, the authors would like to thank CATDS for making available the SMOS datasets which this study would be incomplete without. We would also like to thank Frank Winston and Rodger Young who provided valuable contributions in the installation and maintenance of the soil moisture stations.

Appendix A

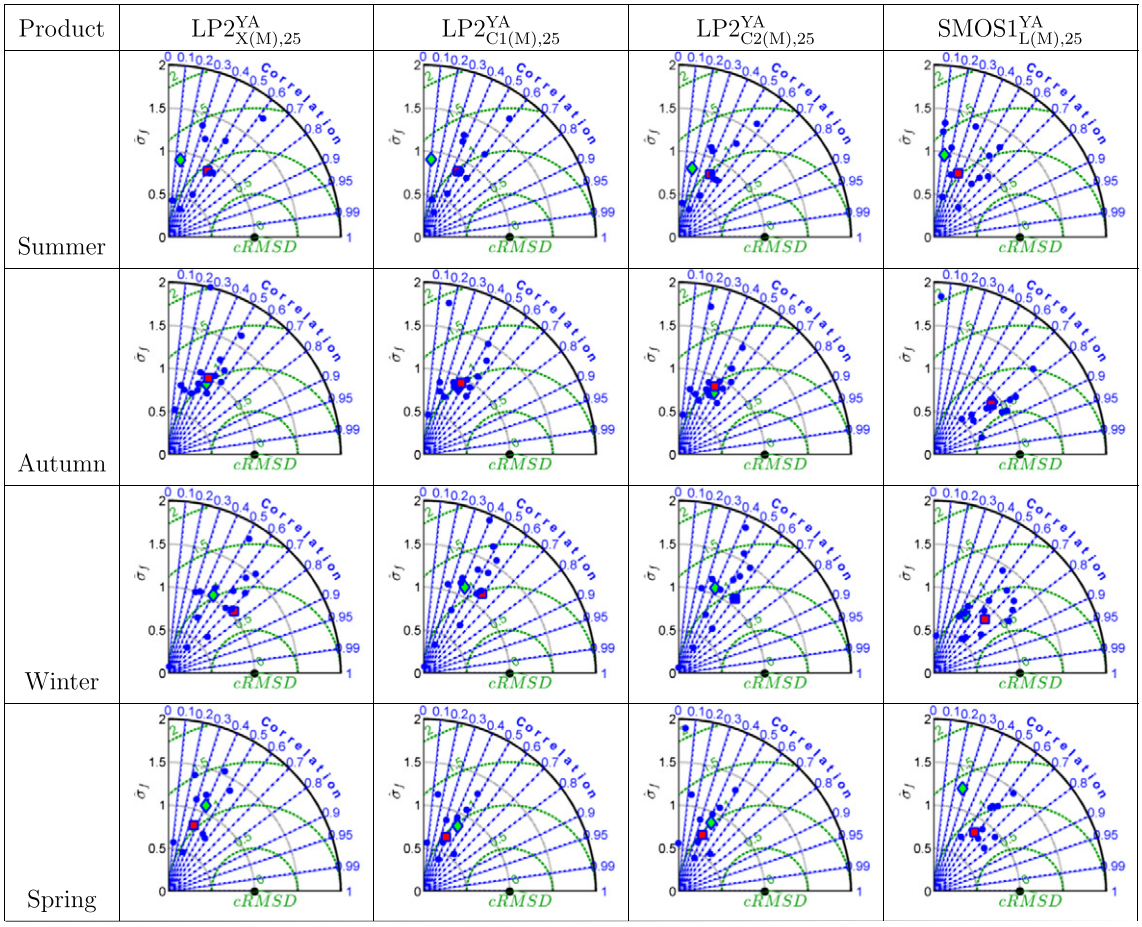

Fig. A1. Taylor diagrams for 25 km grdi resolution morning products in the YA area. Satellite products are treated as the baseline soil moisture (black dot). □: Representative station. ⋄: Average. ◯: Individual stations. Note the difference in scale for JAXA products.

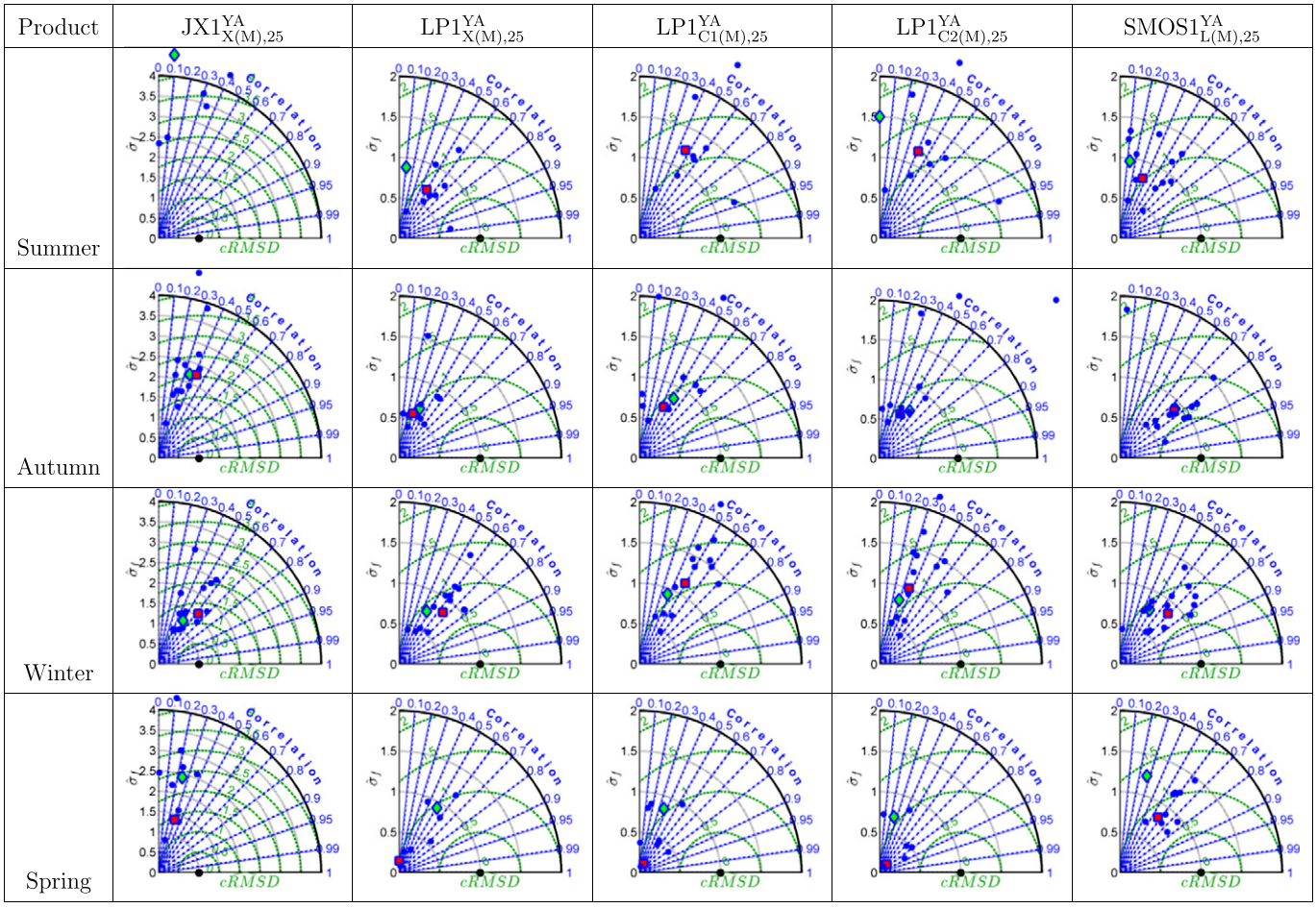

Fig. A2. Taylor diagrams for 25 km grid resolution morning products in the YA area. Satellite products are treated as the baseline soil moisture (black dot). □: Representative station. ⋄: Average. ◯: Individual stations. Note the difference in scale for JAXA products.

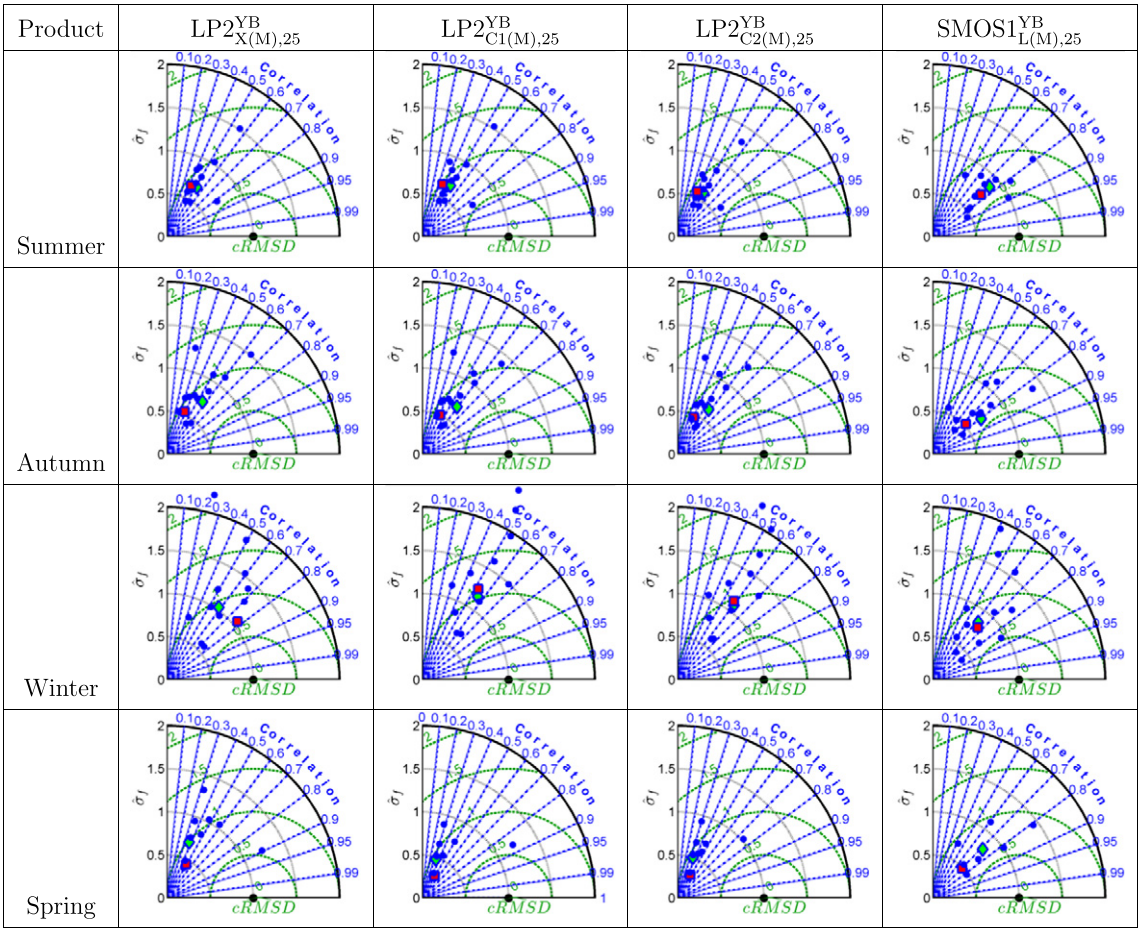

Fig. A3. Taylor diagrams for 25 km grid resolution morning products in the YA area. Satellite products are treated as the baseline soil moisture (black dot). □: Representative station. ⋄: Average. ◯: Individual stations. Note the difference in scale for JAXA products.

Product	$JX1^{YB}_{X(M),25}$	$LP1^{YB}_{X(M),25}$	$LP1^{YB}_{C1(M),25}$	$LP1^{YB}_{C2(M),25}$	$SMOS1^{YB}_{L(M),25}$
Summer	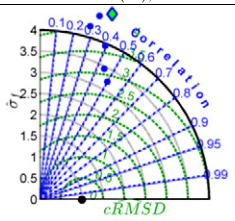	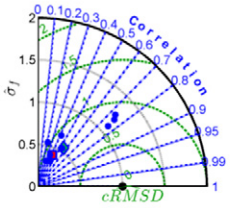	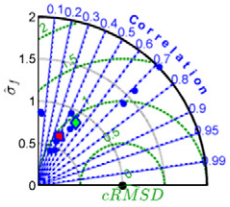	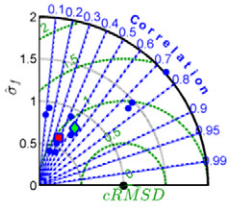	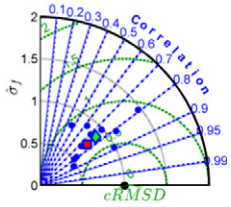
Autumn	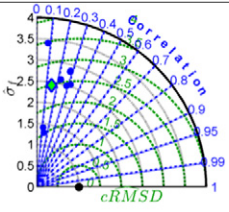	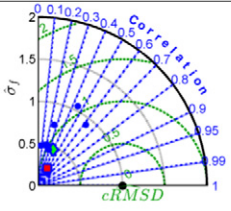	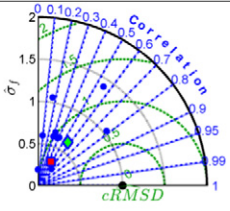	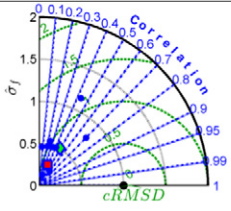	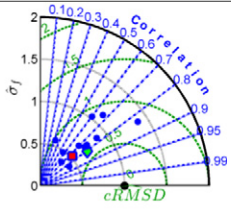
Winter	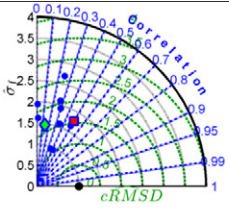	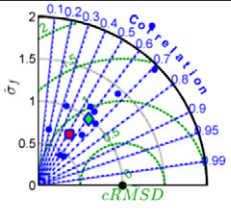	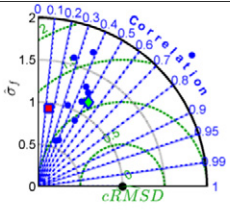	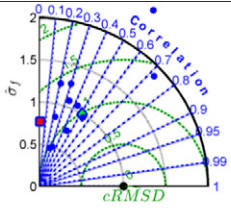	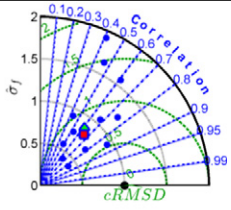
Spring	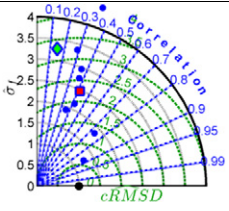	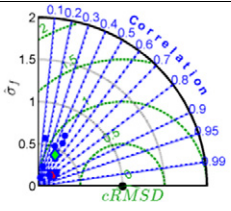	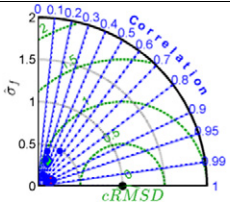	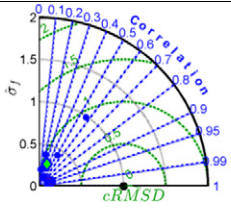	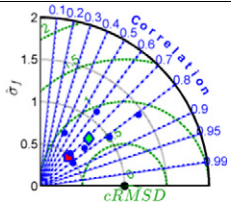

Fig. A4. As Fig. A4 except for YB area.

References

Adams, J.R., McNairn, H., Berg, A.A., Champagne, C., 2015. Evaluation of near-surface soil moisture data from an AAFC monitoring network in Manitoba, Canada: implications for L-band satellite validation. J. Hydrol. 521, 582–592. http://dx.doi.org/10.1016/j.jhydrol.2014.10.024.

Al Bitar, A., Leroux, D., Kerr, Y.H., Merlin, O., Richaume, P., Sahoo, A., Wood, E.F., 2012. Evaluation of SMOS soil moisture products over continental US using the SCAN/SNOTEL network. IEEE Trans. Geosci. Remote Sens. 50, 1572–1586.

Albergel, C., de Rosnay, P., Gruhier, C., Muñoz-Sabater, J., Hasenauer, S., Isaksen, L., Kerr, Y., Wagner, W., 2012. Evaluation of remotely sensed and modelled soil moisture products using global ground-based in situ observations. Remote Sens. Environ. 118, 215–226. http://dx.doi.org/10.1016/j.rse.2011.11.017.

Bindlish, R., Crow, W., Jackson, T., 2009. Role of passive microwave remote sensing in improving flood forecasts. IEEE Geosci. Remote Sens. Lett. 6, 112–116. http://dx.doi.org/10.1109/LGRS.2008.2002754.

Brocca, L., Hasenauer, S., Lacava, T., Melone, F., Moramarco, T., Wagner, W., Dorigo, W., Matgen, P., Martínez-Fernández, J., Llorens, P., Latron, J., Martin, C., Bittelli, M., 2011. Soil moisture estimation through ASCAT and AMSR-E sensors: an intercomparison and validation study across Europe. Remote Sens. Environ. 115, 3390–3408. http://dx.doi.org/10.1016/j.rse.2011.08.003.

Brocca, L., Moramarco, T., Melone, F., Wagner, W., Hasenauer, S., Hahn, S., 2012. Assimilation of surface-and root-zone ASCAT soil moisture products into rainfall - runoff modeling. IEEE Trans. Geosci. Remote Sens. 50, 2542–2555. http://dx.doi.org/10.1109/TGRS.2011.2177468.

Cai, W., Cowan, T., Briggs, P., Raupach, M., 2009. Rising temperature depletes soil moisture and exacerbates severe drought conditions across southeast Australia. Geophys. Res. Lett. 36, http://dx.doi.org/10.1029/2009GL040334.

Champagne, C., Rowlandson, T., Berg, A., Burns, T., L'Heureux, J., Tetlock, E., Adams, J.R., McNairn, H., Toth, B., Itenfisu, D., 2015. Satellite surface soil moisture from SMOS and Aquarius: assessment for applications in agricultural landscapes. Int. J. Appl. Earth Obs. Geoinf. http://dx.doi.org/10.1016/j.jag.2015.09.004.

Cho, E., Moon, H., Choi, M., 2015. First Assessment of the Advanced Microwave Scanning Radiometer 2 (AMSR2) Soil Moisture Contents in Northeast Asia. J. Meteorol. Soc. Japan. Ser. I 93, 117–129. http://ci.nii.ac.jp/naid/130004788805/en/. http://dx.doi.org/10.2151/jmsj.2015-008. Accessed: 2016-10-01.

Choi, M., 2012. Evaluation of multiple surface soil moisture for Korean regional flux monitoring network sites: Advanced Microwave Scanning Radiometer E, land surface model, and ground measurements. Hydrol. Process. 26, 597–603. http://dx.doi.org/10.1002/hyp.8160.

Collow, T.W., Robock, A., Basara, J.B., Illston, B.G., 2012. Evaluation of SMOS retrievals of soil moisture over the central United States with currently available in situ observations. J. Geophys. Res. Atmos. 117, D9. http://dx.doi.org/10.1029/2011JD017095. D09113.

Crow, W.T., Berg, A.A., Cosh, M.H., Loew, A., Mohanty, B.P., Panciera, R., de Rosnay, P., Ryu, D., Walker, J.P., 2012. Upscaling sparse ground-based soil moisture observations for the validation of coarse-resolution satellite soil moisture products. Rev. Geophys. 50, RG2002. http://dx.doi.org/10.1029/2011RG000372.

Crow, W.T., Ryu, D., Famiglietti, J.S., 2005. Upscaling of field-scale soil moisture measurements using distributed land surface modeling. Adv. Water Resour. 28, 1–14. http://dx.doi.org/10.1016/j.advwatres.2004.10.004.

Dall'Amico, J.T., Schlenz, F., Loew, A., Mauser, W., 2012. First results of SMOS soil moisture validation in the upper danube catchment. IEEE Trans. Geosci. Remote Sens. 50, 1507–1516. http://dx.doi.org/10.1109/TGRS.2011.2171496.

Dente, L., Su, Z., Wen, J., 2012a. Validation of SMOS soil moisture products over the Maqu and Twente Regions. Sensors 12, 9965–9986. http://dx.doi.org/10.3390/s120809965.

Dente, L., Vekerdy, Z., Wen, J., Su, Z., 2012b. Maqu network for validation of satellite-derived soil moisture products. Int. J. Appl. Earth Obs. Geoinf. 17, 55–65. http://dx.doi.org/10.1016/j.jag.2011.11.004.

Dirmeyer, P.A., 2000. Using a global soil wetness dataset to improve seasonal climate simulation. J. Climate 13, 2900–2922. http://dx.doi.org/10.1175/1520-0442(2000)013¡2900:UAGSWD¿2.0.CO;2.

Djamai, N., Magagi, R., Goïta, K., Hosseini, M., Cosh, M.H., Berg, A., Toth, B., 2015. Evaluation of SMOS soil moisture products over the CanEx-SM10 area. J. Hydrol. 520, 254–267. http://dx.doi.org/10.1016/j.jhydrol.2014.11.026.

Draper, C.S., 2011. Near-surface Soil Moisture Assimilation in NWP. University of Melbourne, Department of Civil and Environmental Engineering.

Draper, C.S., Walker, J.P., Steinle, P.J., de Jeu, R.A.M., Holmes, T.R.H., 2009. An evaluation of AMSR-E derived soil moisture over Australia. Remote Sens. Environ. 113, 703–710. http://dx.doi.org/10.1016/j.rse.2008.11.011.

Drusch, M., 2007. Initializing numerical weather prediction models with satellite-derived surface soil moisture: data assimilation experiments with ECMWF's integrated forecast system and the TMI soil moisture data set. J. Geophys. Res. Atmos. 112, D3. http://dx.doi.org/10.1029/2006JD007478. D03102.

Du, J., Jackson, T.J., Bindlish, R., Cosh, M.H., Li, L., Hornbuckle, B.K., Kabela, E.D., 2012. Effect of dew on aircraft-based passive microwave observations over an agricultural domain. J. Appl. Remote. Sens. 6, http://dx.doi.org/10.1117/1.JRS.6.063571. 063571–1–063571–10.

Entekhabi, D., Njoku, E.G., O'Neill, P.E., Kellogg, K.H., Crow, W.T., Edelstein, W.N., Entin, J.K., Goodman, S.D., Jackson, T.J., Johnson, J., Kimball, J., Piepmeier, J.R., Koster, R.D., Martin, N., McDonald, K.C., Moghaddam, M., Moran, S., Reichle, R., Shi, J.C., Spencer, M.W., Thurman, S.W., Tsang, L., Van Zyl, J., 2010. The soil moisture active passive (SMAP) mission. Proc. IEEE 98, 704–716. http://dx.doi.org/10.1109/JPROC.2010.2043918.

Escorihuela, M.-J., Chanzy, A., Wigneron, J.-P., Kerr, Y., 2010. Effective soil moisture sampling depth of L-band radiometry: a case study. Remote. Sensing Environ. 114, 995–1001. http://dx.doi.org/10.1016/j.rse.2009.12.011.

Fujii, H., Koike, T., Imaoka, K., 2009. Improvement of the AMSR-E algorithm for soil moisture estimation by introducing a fractional vegetation coverage dataset derived from MODIS data. J. Remote. Sensing Soc. Jpn. 29, 282–292. http://dx.doi.org/10.11440/rssj.29.282.

Griesfeller, A., Lahoz, W.A., Jeu, R., Dorigo, W., Haugen, L.E., Svendby, T.M., Wagner, W., 2015. Evaluation of satellite soil moisture products over Norway using ground-based observations. Int. J. Appl. Earth Obs. Geoinf. 4, http://dx.doi.org/10.1016/j.jag.2015.04.016.

Imaoka, K., Kachi, M., Fujii, H., Murakami, H., Hori, M., Ono, A., Igarashi, T., Nakagawa, K., Oki, T., Honda, Y., Shimoda, H., 2010. Global change observation mission (GCOM) for monitoring carbon, water cycles, and climate change. Proc. IEEE 98, 717–734. http://dx.doi.org/10.1109/JPROC.2009.2036869.

Jackson, T.J., Bindlish, R., Cosh, M.H., Zhao, T., Starks, P.J., Bosch, D.D., Seyfried, M., Moran, M.S., Goodrich, D.C., Kerr, Y.H., Leroux, D., 2012. Validation of Soil Moisture and Ocean Salinity (SMOS) soil moisture over watershed networks in the U.S.. IEEE Trans. Geosci. Remote Sens. 50, 1530–1543. http://dx.doi.org/10.1109/TGRS.2011.2168533.

Jacquette, E., Al Bitar, A., Mialon, A., Kerr, Y., Quesney, A., Cabot, F., Richaume, P., 2010. SMOS CATDS level 3 global products over land. In Remote Sensing Vol. 7824, http://dx.doi.org/10.1117/12.865093. (pp. 78240K–78240K–6).

JAXA, 2015. Release of update AMSR2 products (Version 2.1). Online. http://gcom-w1.jaxa.jp/contents/150403_Ver2.1_release_e.pdf. Accessed: 2016-04-01.

JAXA (n.d.) Data products. http://suzaku.eorc.jaxa.jp/GCOM_W/data/data_w_index.html. http://suzaku.eorc.jaxa.jp/GCOM_W/data/data_w_product-3.html Accessed: 2015-09-03.

Kerr, Y., Waldteufel, P., Richaume, P., Wigneron, J.-P., Ferrazzoli, P., Mahmoodi, A., Al Bitar, A., Cabot, F., Gruhier, C., Juglea, S., Leroux, D., Mialon, A., Delwart, S., 2012. The SMOS soil moisture retrieval algorithm. IEEE Trans. Geosci. Remote Sens. 50, 1384–1403. http://dx.doi.org/10.1109/TGRS.2012.2184548.

Kerr, Y., Waldteufel, P., Wigneron, J.-P., Delwart, S., Cabot, F., Boutin, J., Escorihuela, M.-J., Font, J., Reul, N., Gruhier, C., Juglea, S., Drinkwater, M., Hahne, A., Martin-Neira, M., Mecklenburg, S., 2010. The SMOS mission: new tool for monitoring Key elements of the global qater cycle. Proceedings of the IEEE 98, 666–687. http://dx.doi.org/10.1109/JPROC.2010.2043032.

Kerr, Y.H., Waldteufel, P., Wigneron, J.P., Martinuzzi, J.M., Font, J., Berger, M., 2001. Soil moisture retrieval from space: the Soil Moisture and Ocean Salinity (SMOS) mission. IEEE Trans. Geosci. Remote Sens. 39, 1729–1735. http://dx.doi.org/10.1109/36.942551.

Kim, S., Liu, Y., Johnson, F.M., Parinussa, R.M., Sharma, A., 2015. A global comparison of alternate AMSR2 soil moisture products: why do they differ? Remote Sens. Environ. 161, 43–62. http://dx.doi.org/10.1016/j.rse.2015.02.002.

Lacava, T., Faruolo, M., Pergola, N., Coviello, I., Tramutoli, V., 2012. A comprehensive analysis of amsre c- and x-bands radio frequency interferences. Microwave Radiometry and Remote Sensing of the Environment (MicroRad), 2012 12th Specialist Meeting on. pp. 1–4. http://dx.doi.org/10.1109/MicroRad.2012.6185256.

Maeda, T., Imaoka, K., Kachi, M., Fujii, H., Shibata, A., Naoki, K., Kasahara, M., Ito, N., Nakagawa, K., Oki, T., 2011. Status of GCOM-W1/AMSR2 development, algorithms, and products. Proc. SPIE 8176, http://dx.doi.org/10.1117/12.898381. 81760N–81760N–7.

Maeda, T., Taniguchi, Y., 2013. Descriptions of GCOM-W1 AMSR2 Level 1R and Level 2 algorithms. Online. http://suzaku.eorc.jaxa.jp/GCOM_W/data/doc/NDX-120015A.pdf. nDX-120015A.

McKenzie, N.J., Jacquier, D., Ashton, L., Cresswell, H., 2000. Estimation of Soil Properties using the Atlas of Australian Soils. CSIRO Land and Water Canberra.

Merlin, O., Walker, J.P., Kalma, J.D., Kim, E.J., Hacker, J., Panciera, R., Young, R., Summerell, G., Hornbuckle, J., Hafeez, M., Jackson, T., 2008. The NAFE06 data set: towards soil moisture retrieval at intermediate resolution. Adv. Water Res. 31, 1444–1455. http://dx.doi.org/10.1016/j.advwatres.2008.01.018.

Mo, T., Choudhury, B.J., Schmugge, T.J., Wang, J.R., Jackson, T.J., 1982. A model for microwave emission from vegetation-covered fields. J. Geophys. Res. Oceans 87, 11229–11237. http://dx.doi.org/10.1029/JC087iC13p11229.

Naeimi, V., Bartalis, Z., Wagner, W., 2009. ASCAT soil moisture: an assessment of the data quality and consistency with the ERS scatterometer heritage. J. Hydrometeorol. 10, 555–563. http://dx.doi.org/10.1175/2008JHM1051.1.

de Nijs, A., Parinussa, R., de Jeu, R., Schellekens, J., Holmes, T., 2015. A methodology to determine radio-frequency interference in amsr2 observations. IEEE Trans. Geosci. Remote Sens. 53, 5148–5159. http://dx.doi.org/10.1109/TGRS.2015.2417653.

Njoku, E., Li, L., 1999. Retrieval of land surface parameters using passive microwave measurements at 6–18 GHz. IEEE Trans. Geosci. Remote Sens. 37, 79–93. http://dx.doi.org/10.1109/36.739125.

Njoku, E.G., Ashcroft, P., Chan, T.K., Li, L., 2005. Global survey and statistics of radio-frequency interference in AMSR-E land observations. IEEE Trans. Geosci. Remote Sens. 43, 938–947. http://dx.doi.org/10.1109/TGRS.2004.837507.

Owe, M., De Jeu, R., Walker, J., 2001. A methodology for surface soil moisture and vegetation optical depth retrieval using the microwave polarization difference index. IEEE Trans. Geosci. Remote Sens. 39, 1643–1654.

Owe, M., de Jeu, R., Holmes, T., 2008. Multisensor historical climatology of satellite-derived global land surface moisture. J. Geophys. Res. F: Earth Surf. 113, F1. http://dx.doi.org/10.1029/2007JF000769.

Panciera, R., Walker, J.P., Jackson, T.J., Gray, D.A., Tanase, M.A., Ryu, D., Monerris, A., Yardley, H., Rüdiger, C., Wu, X., Gao, Y., Hacker, J.M., 2014. The Soil Moisture

Active Passive Experiments (SMAPEx): toward soil moisture retrieval from the SMAP mission. IEEE Trans. Geosci. Remote Sens. 52, 490–507. http://dx.doi.org/10.1109/TGRS.2013.2241774.

Parinussa, R.M., Holmes, T.R.H., Wanders, N., Dorigo, W.A., de Jeu, R.A.M., 2015. A preliminary study toward consistent soil moisture from AMSR2. Journal of Hydrometeorol. 16, 932–947. http://dx.doi.org/10.1175/JHM-D-13-0200.1.

Peischl, S., Walker, J.P., Rüdiger, C., Ye, N., Kerr, Y.H., Kim, E., Bandara, R., Allahmoradi, M., 2012. The AACES field experiments: SMOS calibration and validation across the Murrumbidgee River catchment. Hydrol. Earth Syst. Sci. 16, 1697–1708. http://dx.doi.org/10.5194/hess-16-1697-2012.

Raju, S., Chanzy, A., Wigneron, J.-P., Calvet, J.-C., Kerr, Y., Laguerre, L., 1995. Soil moisture and temperature profile effects on microwave emission at low frequencies. Remote Sens. Environ. 54, 85–97. http://dx.doi.org/10.1016/0034-4257(95)00133-L.

Rötzer, K., Montzka, C., Bogena, H., Wagner, W., Kerr, Y.H., Kidd, R., Vereecken, H., 2014. Catchment scale validation of SMOS and ASCAT soil moisture products using hydrological modeling and temporal stability analysis. J. Hydrol. 519, 934–946. http://dx.doi.org/10.1016/j.jhydrol.2014.07.065.

Rowlandson, T.L., Hornbuckle, B.K., Bramer, L.M., Patton, J.C., Logsdon, S.D., 2012. Comparisons of evening and morning SMOS passes over the Midwest United States. IEEE Trans. Geosci. Remote Sens. 50, 1544–1555. http://dx.doi.org/10.1109/TGRS.2011.2178158.

van der Schalie, R., Parinussa, R.M., Renzullo, L.J., van Dijk, A., Su, C.-H., de Jeu, R.A.M., 2015. SMOS soil moisture retrievals using the land parameter retrieval model: evaluation over the Murrumbidgee Catchment, southeast Australia. Remote Sens. Environ. 163, 70–79. http://dx.doi.org/10.1016/j.rse.2015.03.006.

Schmugge, T.J., Kustas, W.P., Ritchie, J.C., Jackson, T.J., Rango, A., 2002. Remote sensing in Hydrology. Adv. Water Res. 25, 1367–1385. http://dx.doi.org/10.1016/S0309-1708(02)00065-9.

Seneviratne, S.I., 2010. Investigating soil moisture-climate interactions in a changing climate: a review. Earth Sci. Rev. 99, 99–174. http://dx.doi.org/10.1016/j.earscirev.2010.02.004.

Smith, A.B., Walker, J.P., Western, A.W., Young, R.I., Ellett, K.M., Pipunic, R.C., Grayson, R.B., Siriwardena, L., Chiew, F.H.S., Richter, H., 2012. The Murrumbidgee soil moisture monitoring network data set. Water Resour. Res. 48, W07701. http://dx.doi.org/10.1029/2012WR011976.

Su, C.H., Ryu, D., Young, R.I., Western, A.W., Wagner, W., 2013. Inter-comparison of microwave satellite soil moisture retrievals over the Murrumbidgee Basin, southeast Australia. Remote Sens. Environ. 134, 1–11. http://dx.doi.org/10.1016/j.rse.2013.02.016.

Taylor, K.E., 2001. Summarizing multiple aspects of model performance in a single diagram. J. Geophys. Res. Atmospheres 106, 7183–7192. http://dx.doi.org/10.1029/2000JD900719.

Wagner, W., Hahn, S., Kidd, R., Melzer, T., Bartalis, Z., Hasenauer, S., Figa-Saldaña, J., de Rosnay, P., Jann, A., Schneider, S., Komma, J., Kubu, G., Brugger, K., Aubrecht, C., Züger, J., Gangkofner, U., Kienberger, S., Brocca, L., Wang, Y., Blöschl, G., Eitzinger, J., Steinnocher, K., Zeil, P., Rubel, F., 2013. The ASCAT soil moisture product: a review of its specifications, validation results, and emerging applications. Meteorol. Z. 22, 5–33. http://dx.doi.org/10.1127/0941-2948/2013/0399.

Wen, J., Su, Z., 2003. A time series based method for estimating relative soil moisture with ERS wind scatterometer data. Geophysical.Res. Lett. 30, 1397. http://dx.doi.org/10.1029/2002GL016557. 1397.

Wigneron, J.-P., Kerr, Y., Waldteufel, P., Saleh, K., Escorihuela, M.-J., Richaume, P., Ferrazzoli, P., de Rosnay, P., Gurney, R., Calvet, J.-C., Grant, J., Guglielmetti, M., Hornbuckle, B., Mätzler, C., Pellarin, T., Schwank, M., 2007. L-band Microwave Emission of the Biosphere (L-MEB) Model: description and calibration against experimental data sets over crop fields. Remote Sens. Environ. 107, 639–655. http://dx.doi.org/10.1016/j.rse.2006.10.014.

Wu, Q., Liu, H., Wang, L., Deng, C., 2015. Evaluation of AMSR2 soil moisture products over the contiguous United States using in situ data from the International Soil Moisture Network. Int. J. Appl. Earth Obs. Geoinf. 45, 187–199. http://dx.doi.org/10.1016/j.jag.2015.10.011.

Yee, M.S., Walker, J.P., Monerris, A., Rüdiger, C., Jackson, T.J., 2016. On the identification of representative in situ soil moisture monitoring stations for the validation of SMAP soil moisture products in Australia. J. Hydrol. http://dx.doi.org/10.1016/j.jhydrol.2016.03.060. Available online 2 April 2016.

Zeng, J., Li, Z., Chen, Q., Bi, H., Qiu, J., Zou, P., 2015. Evaluation of remotely sensed and reanalysis soil moisture products over the Tibetan plateau using in-situ observations. Remote Sensing of Environment 163, 91–110. http://dx.doi.org/10.1016/j.rse.2015.03.008.

Zhang, H., Pak, B., Wang, Y.P., Zhou, X., Zhang, Y., Zhang, L., 2013. Evaluating surface water cycle simulated by the Australian community land surface model (CABLE) across different spatial and temporal domains. J. Hydrometeorol. 14, 1119–1138. http://dx.doi.org/10.1175/jhm-d-12-0123.1.